Eye movements elevate crowding in congenital idiopathic nystagmus

Vijay K Tailor[1,2,3], Maria Theodorou[2,3], Annegret H Dahlmann-Noor[2,3], Tessa M Dekker[1,2], & John A Greenwood[1]

[1] Experimental Psychology, University College London, London, UK
[2] NIHR Biomedical Research Centre @ Moorfields Eye Hospital and UCL Institute of Ophthalmology, London, UK
[3] Moorfields Eye Hospital NHS Foundation Trust, London, UK

Keywords

Nystagmus, Amblyopia, Visual Crowding, Eye Movements, Spatial Vision

Corresponding author: Vijay K. Tailor
Email: vijay.tailor.09@ucl.ac.uk

Abstract

Congenital idiopathic nystagmus (sometimes known as infantile nystagmus) is a disorder characterised by involuntary eye movements, which leads to decreased acuity and visual function. One such function is visual crowding, a process whereby objects that are easily recognised in isolation become impaired by nearby flankers. Crowding typically occurs in the peripheral visual field, though elevations in foveal vision have been reported in congenital nystagmus, similar to those found with amblyopia (another developmental visual disorder). Here we examine whether the elevated foveal crowding with nystagmus is driven by similar mechanisms to those documented in amblyopia – long-term neural changes associated with a sensory deficit – or by the momentary displacement of the stimulus through nystagmus eye movements. We used a Landolt-C orientation identification task to measure threshold gap sizes with and without flanker Landolt-Cs that were either horizontally or vertically placed. Because nystagmus is predominantly horizontal, crowding should be stronger with horizontal flankers if eye movements cause the interference, whereas a sensory deficit should be equivalent for the two dimensions. Consistent with an origin in eye movements, we observe elevations in nystagmic crowding that are above that of typical vision, and stronger with horizontal than vertical flankers. This horizontal elongation was not found in either amblyopic or typical vision. We further demonstrate that the same pattern of performance can be obtained in typical vision with stimulus movement that simulates nystagmus. We consequently propose that the origin of nystagmic crowding lies in the eye movements, either through relocation of the stimulus into peripheral retina or image smear of the target and flanker elements.

Introduction

Our eyes are in constant motion. For some people, this motion is exaggerated and uncontrollable, a condition known as nystagmus that can be either congenital or acquired (Papageorgiou, McLean, & Gottlob, 2014). Congenital or infantile nystagmus typically has an onset prior to 6-months of age and can be idiopathic (i.e. of no known cause), or related to a visual afferent abnormality - retinal dystrophies, albinism, low-vision, visual deprivation or a plethora of neurological conditions (Papageorgiou et al., 2014). Congenital infantile nystagmus has an incidence of 14 per 10,000 population, with congenital idiopathic nystagmus estimated at 1.9 per 10,000 population (Sarvananthan et al., 2009). Nystagmus eye movements are predominantly horizontal in direction, with occasional oscillations in the vertical and torsional plane (Abadi & Bjerre, 2002). Areas of visual function that are often reduced with nystagmus include visual acuity (Abadi & Bjerre, 2002), stereo-acuity (Guo, Reinecke, Fendick, & Calhoun, 1989; Ukwade & Bedell, 1999) and contrast sensitivity (Dickinson & Abadi, 1985). Particularly disruptive for foveal vision are the elevations in crowding, whereby objects that are easily recognised in isolation become impaired by nearby flankers (Chung & Bedell, 1995; Pascal & Abadi, 1995).

Crowding is a phenomenon that occurs in the peripheral visual field of typically/normal sighted people, disrupting the identification but not the detection of a target stimulus in clutter (Levi, Hariharan, & Klein, 2002b, 2002c; Pelli, Palomares, & Majaj, 2004). These disruptions to object recognition occur over and above acuity limitations – an object can be large enough to overcome acuity limitations and yet still be difficult to recognise once flankers are placed around it (Pelli et al., 2004). The spatial extent of crowding can be quantified by measuring the transition point (or critical spacing) between largely correct and incorrect identification of the target. At an eccentricity of $\phi°$, Bouma (1970) found this spacing to be a distance of $0.5\times \phi°$ – for example, a target at 6° eccentricity would be crowded by objects up to 3° away. The resulting increase in crowding with eccentricity gives large spatial extents for crowding in peripheral vision (Toet & Levi, 1992) particularly in comparison to foveal crowding, where it typically affects only a small area of approximately 4-5 minutes of arc (Coates, Levi, Touch, & Sabesan, 2018; Flom, Heath, & Takahashi, 1963; Liu & Arditi, 2000).

In peripheral vision, the spatial extent of crowding shows a number of variations in both size and shape. For instance, flankers positioned outward from the target (with respect to fixation) have a greater effect on identification than inward flankers (Bouma, 1970). Toet and Levi (1992) further demonstrated a radial-tangential anisotropy, where the critical spacing is greater for flankers along the radial dimension compared to the tangential dimension relative to fixation. Variations have also been observed around the visual field, including the upper-lower anisotropy where crowding is stronger in the upper compared to the lower visual field (Greenwood, Szinte, Sayim, & Cavanagh, 2017; Petrov & Meleshkevich, 2011). In addition to the radial-tangential anisotropy, it has also been found that horizontally placed flankers induce more crowding than vertically placed flankers in the 4 quadrants of the peripheral visual field (Feng, Jiang, & He, 2007). In contrast to peripheral vision, foveal interaction zones have been found to be more circular, with equivalent crowding in the

horizontal and vertical dimensions in typical vision (Flom et al., 1963; Toet & Levi, 1992) and for the elevations in the amblyopic fovea (Levi & Carney, 2011).

Elevations in the extent of visual crowding have been demonstrated in the foveal vision of those with strabismic amblyopia Levi (2008). This developmental disorder occurs through a misalignment in the visual axis, disrupting retinal correspondence and leading to a reduction in acuity with the deviating eye (Barrett, Bradley, & McGraw, 2004; McKee, Levi, & Movshon, 2003). Amblyopic crowding exhibits many of the same attributes as peripheral crowding (**cite Levi, Hariharan, & Klein, 2002c) and has been exhibited in both children and adults (Greenwood et al., 2012; Levi & Klein, 1985), causing clear disruption to reading with the amblyopic fovea. There is also evidence for a common mechanism in these instances. In peripheral vision, crowding produces systematic errors that are well described by a population coding process that inappropriately combines features from target and flanker elements (Greenwood, Bex, & Dakin, 2009; Harrison & Bex, 2015; Parkes, Lund, Angelucci, Solomon, & Morgan, 2001). A similar process has recently been found to account for errors in the amblyopic fovea due to crowding (Kalpadakis-Smith, Tailor, Dahlmann-Noor, & Greenwood, 2017). Amblyopic elevations have been linked to a sensory deficit with a reduction in the number of neurons driven by the amblyopic eye (Kiorpes & McKee, 1999) and increases in receptive field size (Clavagnier, Dumoulin, & Hess, 2015) in cortical areas V1 and above.

In the case of nystagmus, it is far less clear whether the associated deficits in visual function reflect a sensory deficit associated with long-term neural changes, or a momentary disruption associated with the movement of the eyes. The most widely studied visual function in this context is the decrease in visual acuity associated with nystagmus (Cesarelli, Bifulco, Loffredo, & Bracale, 2000), which has been shown to correlate with the amount of time spent with the stimulus under foveation (Abadi & Worfolk, 1989; Bedell, 2000; Dell'Osso, 2002; Dell'Osso & Jacobs, 2002; Dell'Osso, van der Steen, Steinman, & Collewijn, 1992; Theodorou, 2006). Foveation periods are defined as phases when eye movements are slow, with the fovea in close proximity to the stimulus. However, if eye movements and reduced foveation time were the sole cause of nystagmic deficits, then the disruptions to visual function should vary by the configuration of the elements, with elements arranged along the horizontal axis likely to be most disrupted as they smear together due to the predominantly horizontal eye movements. Ukwade and Bedell (2012) found a similar pattern of elevation for bisection acuity, with greater elevation for horizontal judgements than vertical in individuals with congenital nystagmus. However, thresholds for *both* horizontal and vertical elements were elevated relative to control participants, suggesting that at least part of the impairment in visual function may derive from a sensory neural deficit, as in amblyopia.

Although the elevation of foveal crowding in nystagmus has been clearly demonstrated (Chung & Bedell, 1995; Pascal & Abadi, 1995), the underlying basis for these deficits remains unclear – in particular, whether they derive from a sensory deficit (as in amblyopia) or through the involuntary eye movements. Pascal and Abadi (1995) examined participants with idiopathic nystagmus, albinism and typical vision. Acuity was measured using oriented Landolt-Cs, with crowding induced using flanker bars. Crowding was elevated in both the

idiopathic and albino groups compared to the controls, though this difference was only significant for the idiopaths. The authors attributed these results to the difference in eye movements between the two groups, with the jerk movements in idiopaths being more disruptive to thresholds than the pendular eye movements in albinism. The implication is that image motion caused by eye movements may be the primary determinant of nystagmic crowding.

On the other hand, Chung and Bedell (1995) present evidence that the elevations in the spatial extent of crowding for nystagmats derives from a sensory deficit. Chung and Bedell (1995) examined acuity with isolated Landolt-C targets and induced crowding with a black or white surround. For participants with nystagmus, crowding was elevated relative to controls with both the white and black surrounds. In order to test the role of stimulus motion on these crowding effects, Chung and Bedell (1995) applied a simulated and repetitive jerk nystagmus movement to the stimulus in a group with typical vision. The repetitive waveform movements resulted in reduced acuity and elevated crowding compared to the stationary acuity measurement. However, these simulated deficits in acuity and crowding did not reach the same level of impairment as the nystagmus participants, suggesting that eye movements alone are insufficient and that an underlying sensory deficit may be required to explain the remainder of the deficit, similar to that seen in amblyopia.

It is unclear from these studies whether crowding in nystagmus originates from either the momentary image smear caused by eye movements or an underlying sensory deficit. Here, we sought to investigate the mechanisms behind these elevations in crowding in participants with nystagmus, and their origin. To do so, we measured the spatial extent of crowding in congenital idiopathic nystagmus with flankers placed either horizontally or vertically relative to a target Landolt-C element. Because nystagmus eye movements are predominantly along the horizontal dimension, factors related to these eye movements such as image smear should lead to horizontally-placed flankers causing the most disruption. If nystagmic crowding derives from momentary eye movements, we should therefore find a horizontal elongation of the spatial extent of crowding region in participants with congenital nystagmus, with far less effect for vertical flankers. In contrast, if nystagmic crowding derives from a sensory deficit associated with factors such as an increase in receptive field size, then the elevation in crowding should be equivalent for the two dimensions, as observed in amblyopia (Levi & Carney, 2011). In order to examine the effect of nystagmus in participants with no observable retinal or neural defects, we examined those with congenital idiopathic nystagmus. We compared this group to adults with strabismic amblyopia, a population where crowding is more clearly derived from a sensory deficit, as well as participants with typical vision.

To foreshadow the results, in Experiment 1, we find elevations in nystagmic crowding that are greater with horizontally placed flankers than with vertically placed flankers, matching the horizontal bias in their eye movements. These elevations in the spatial extent of crowding and the horizontal-elongation of crowding can be replicated in typical vision when nystagmus movement patterns are applied to stimuli, as we show in Experiment 2. We propose that nystagmus eye movements increase foveal crowding either through a relocation of the stimuli onto peripheral

retina or through image smear of the target and flanker elements.

Experiment 1: Crowding with horizontal and vertical flankers

Methods

Participants

Thirty-one adults underwent a full orthoptic examination to ensure they met inclusion and exclusion criteria into one of three clinical groups: nystagmus (n = 8, M_{age} = 30.3 years), strabismic amblyopia (n = 10, M_{age} = 36.2 years) or controls (n = 10, M_{age} = 32.1 years). All participants were between the ages of 19-49 years old with no neurological conditions. Control participants had to achieve a best corrected visual acuity (BCVA) in each eye of 0.20 logMAR or better, with no strabismus or nystagmus present. In the amblyopic group, participants needed to demonstrate strabismic or mixed amblyopia with manifest strabismus, as well as a BCVA difference of 0.20 logMAR between the two eyes, a BCVA in the amblyopic eye between 0.20 and 1.00 logMAR, and a BCVA of 0.20 logMAR or better in the fellow eye. For the nystagmus group a horizontal, vertical or torsional nystagmus waveform had to be present with a diagnosis of idiopathic nystagmus (without visual afferent abnormality), a BCVA of 1.00 logMAR or better and no manifest strabismus. Three adults with nystagmus were excluded due to an incorrect nystagmus diagnosis and are not included in the above tally.

Clinical characteristics can be found in Appendix 1. BCVA was measured using a logMAR chart, with a mean visual acuity (±1 SD) for the control group of -0.09 ±0.11 logMAR, 0.56 ±0.28 logMAR for the amblyopic group, and 0.29 ±0.26 logMAR for the nystagmic group. Controls all demonstrated excellent stereo-acuity (measured with the Frisby stereo-test), with no ocular motility imbalances. Amblyopes all had a predominantly horizontal strabismus, with 2/10 exhibiting a small vertical component, and no stereopsis demonstrated in any case. Nystagmats all showed nystagmus eye movements that were predominantly horizontal in direction, and which involved either a jerk or pendular movement. No strabismus was present and stereopsis was found in all cases, with a mean stereo-acuity of 350 seconds of arc.

Apparatus

Testing was undertaken at Moorfields Eye Hospital, London. Experiments were programmed using Matlab (The Mathworks, Ltd.) on a Dell PC running PsychToolBox (Brainard, 1997; Pelli, 1997). Stimuli were presented on an Eizo Flexscan EV2736W LCD monitor, with 2560 × 1440-pixel resolution, 60Hz refresh rate, and a physical panel size of 59.7 × 33.6 cm. Monitor calibration was undertaken using a Minolta photometer, with monitor luminance linearised in software to give a maximum luminance of 150 cd/m^2. Participant responses to stimuli were indicated by a keypad. An EyeLink 1000 (SR research, Ottawa, Canada) recorded the position of the dominant eye at a sampling rate of 1000 Hz. Participants had their head positioned on a chin rest with a forehead bar to minimise head movement. Stimulus presentation was monocular, achieved through occlusion of either the non-amblyopic eye for amblyopes or the non-dominant eye for controls. Data was analysed in Matlab and SPSS.

Stimuli and procedures

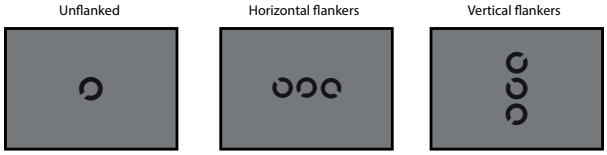

Figure 1. Examples of the Landolt-C discrimination task, unflanked (single presentation of a Landolt-C), flanked-horizontal (participants choose the orientation of the middle Landolt-C, flanked horizontally by two other Landolt-C elements) and flanked-vertical.

Target and flanker stimuli were Landolt-C letters presented at the centre of the screen, either in isolation (unflanked) or flanked by two Landolt-C elements positioned either horizontally or vertically. Elements were presented at 100% Weber contrast against a mid-grey background (Figure 1). Participants identified the position of the gap of the Landolt-C (four alternative forced choice, 4AFC). The orientation of the Landolt-C was always oblique, either at 45°, 135°, 225°, or 315°. These oblique orientations were selected following pilot testing (by authors VKT and JAG) with gap orientations at cardinal positions (0°, 90°, 180° and 270°), where we found improved identification of orientation when target gap orientations were orthogonal to the flankers (e.g. up/down gap orientation was better when horizontal flankers were present and vice versa). On modification of the orientation to oblique positions we found the identification of gap orientation to be equivalent across all configurations. Stimuli were presented with unlimited duration until a response was made, at which point they were removed from the screen. A 500ms inter-trial interval with a blank screen (leaving only fixation) was then presented prior to the next stimulus. Feedback on choice was not given. Participants were encouraged to make a choice in a timely manner.

The gap size and stroke width of Landolt-C elements was 1/5th of the diameter, which was scaled using an adaptive QUEST procedure (Watson & Pelli, 1983). Target and flanker Landolt-C sizes were scaled using the QUEST which converged on 62.5% correct responses (midway between chance and 100% correct). To avoid rapid convergence of the QUEST we added variance to the gap sizes presented, which minimised the number of trials presented at the same size. Variance was calculated on each trial by shifting the gap size value requested by the QUEST algorithm by a value selected from a Gaussian distribution centred on 0 which was multiplied by 0.25 of the current trial estimate of the threshold. This variance was used to improve the subsequent fit of psychometric functions to the data, as found previously (Kalpadakis-Smith, Tailor, Dahlmann-Noor, Schwarzkopf, & Greenwood, 2018). When flankers were present, their centre-to-centre separation from the target was 1.1 times the size of the target, following Song, Levi, and Pelli (2014) who found this to be the ideal spacing to measure crowding effects in normal peripheral vision and the amblyopic fovea. Flanker sizes matched the target.

Participants were allowed to undertake 5 practice trials (identifying the orientation of the gap of the target Landolt-C) at the start of each block of trials so they understood the task. In total 65 trials were undertaken in each block, including the 5 practice trials, which were not included in the main analysis. We undertook 4 repeats of each block, with a total of 240 trials (excluding practice trials) for each stimulus condition (unflanked, horizontal flankers and vertical flankers). The whole experiment was undertaken in 2 hours, which participants undertook over a number of sessions.

Ethics was obtained from the NHS North Thames Research Ethics Committee and participants were pseudonymised following informed consent being obtained. Participants were reimbursed for their time and travel expenses.

Eye tracking

Eye movements were recorded with the EyeLink 1000 to characterise the nystagmus eye movements and to monitor participant gaze throughout the trials. Calibration was undertaken at the beginning of each block of trials, with amblyopic and control participants calibrated using the EyeLink 1000 inbuilt 5-point calibration routine. Calibration for amblyopes was performed with the amblyopic eye and the dominant eye in the controls.

Several of the participants with nystagmus could not undertake the inbuilt EyeLink calibration process due to the large variability in their eye position. The nystagmus participants were thus calibrated using a novel 5-point system, similar to several procedures reported recently for the calibration of participants with nystagmus (Dunn et al., 2019; Rosengren, Nyström, Hammar, & Stridh, 2020). Prior to this calibration, an observer with typical vision undertook the inbuilt EyeLink calibration process, which allowed the EyeLink to identify the parameters of the screen in relation to the eye tracker. For our custom calibration, white circles were then presented at fixation targets with a diameter of 0.5° and a brightness of 150 cd/m^2. These were presented binocularly in a random order at the centre of the screen and separated by 5° at the following positions – 0°, 90°, 180°, 270°. The participant was instructed to look at the fixation target for 5 seconds and move to the new location. EyeLink recordings were observed by the examiner and if a loss of recording or excessive blinking was detected the calibration was repeated.

Calibration recordings were used to undertake a post-hoc calibration of eye position using a geometric transformation. Data from the first 0.5 seconds of each calibration trial location was first discarded to allow for fixation to arrive on the target. We next removed any time points where the velocity of the eye was more than ±1SD from the mean velocity of the eye across the whole trial, leaving only the positions of the eye where the velocity was slow. The mean of these slow phases became our fixation locations for each of the five calibration target locations. These values were compared to the calibration target locations on the screen, with an affine geometric transformation used to align the two sets of points. This transformation was chosen after pilot testing as best able to preserve the ratios of the distances between the points lying on a straight line to give the final geometric transformation value. This transformation value was then applied to the eye positions recorded within the main trials of the experiment. Each block of trials had a corresponding calibration file as head position may have varied between blocks of trials. Difficulties were found with one nystagmus participant where one calibration file was unable to constrain the affine geometric transformation value. To overcome this, we applied the affine geometric transformation from a prior block of trials.

Once the affine geometric transformation was calculated and applied to all corresponding trials the final processing of the eye fixation was undertaken. Blinks were removed following identification through absent pupil readings. Blink generation was also removed by identifying readings within 150 milliseconds before and after the blink, as determined during pilot testing.

For all participants, eye positions within each trial were converted to error values around the fixation in degrees of visual angle. At each timepoint, velocity was computed as a moving estimate of 3 successive eye-position samples in order to reduce noise within the velocity calculations (Engbert & Kliegl, 2003).

Results

Behavioural results

For each participant and stimulus condition (unflanked, horizontal flankers and vertical flankers), the four blocks of 60 trials were combined to give 240 trials per stimulus condition. For each stimulus size that was presented, the corresponding proportion correct scores for responses were then collated. Psychometric functions were fitted to the behavioural data for each stimulus condition by using a cumulative Gaussian function with 3 free parameters (midpoint, slope and lapse rate). Because the variability added to the QUEST gave variable trial numbers for each gap size, this fitting was performed by weighting the least-squared error value by the number of trials per point. Figure 2A plots example proportion correct values for one nystagmus participant in the unflanked condition (green circles) along with the best-fitting psychometric function (black line). Figure 2B and 2C show data for the horizontal flanker (blue circles) and vertical flanker (red circles) conditions. Note that with the variable number of trials for each gap size that some proportion correct values can lie at the extremes due to a low number of trials (e.g. the lowest value in Figure 2B, which derives from a single trial), but that the weighted function fitting de-emphasises these values. Gap-size thresholds were derived from the psychometric function when performance reached 62.5% correct (mid-way between chance and ceiling), and converted to degrees of visual angle.

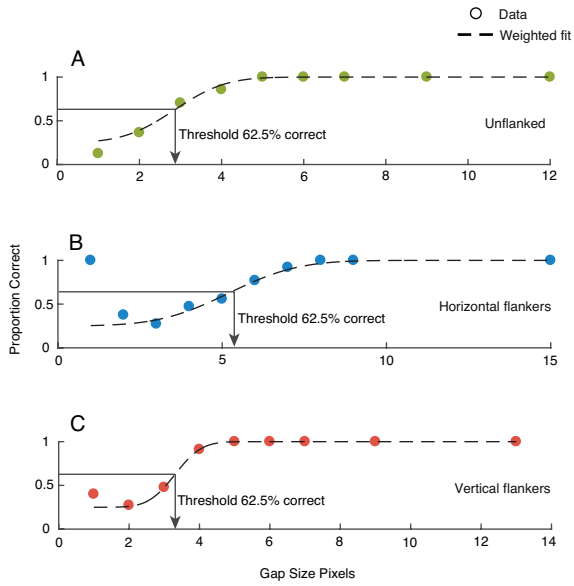

Figure 2. A-C. Example data for the 3 stimulus conditions (unflanked, horizontal flankers and vertical flankers) in a patient with nystagmus. Circles plot the proportion of correct responses at each of the gap sizes presented. The black dashed line plots the best-fitting psychometric function. Thresholds were taken at 62.5% correct, shown as the black solid line and its corresponding threshold on the x-axis (here, in pixels). Note the different scales along the x-axes.

Figure 3A plots the mean gap thresholds for all participant groups. In the control group, gap thresholds were low overall in all stimulus conditions with the unflanked condition (green bar) having the lowest threshold and rising slightly with either horizontal flankers (blue bar) or vertical flankers (red bar). The amblyopic group demonstrated large elevations of gap thresholds in all tasks compared to the control group, particularly when crowded. Finally, thresholds for the nystagmus group were elevated in all conditions compared to the control group, though to a lesser extent than the amblyopic group.

We undertook a 3x3 mixed effects ANOVA to further examine these differences, with factors for participant group and stimulus condition. A main

effect of stimulus condition was found ($F_{(2,50)}$ = 8.779, p=0.001), indicating that the presence of flankers affected the gap thresholds. The main effect of participant group was not significant ($F_{(2,25)}$ = 5.560, p=0.100), though there was a significant interaction between stimulus condition and participant group ($F_{(4,50)}$ = 4.638, p=0.003). This indicates that the effect of stimulus condition on gap thresholds differed for the participant groups, which we examined with a series of a priori contrasts.

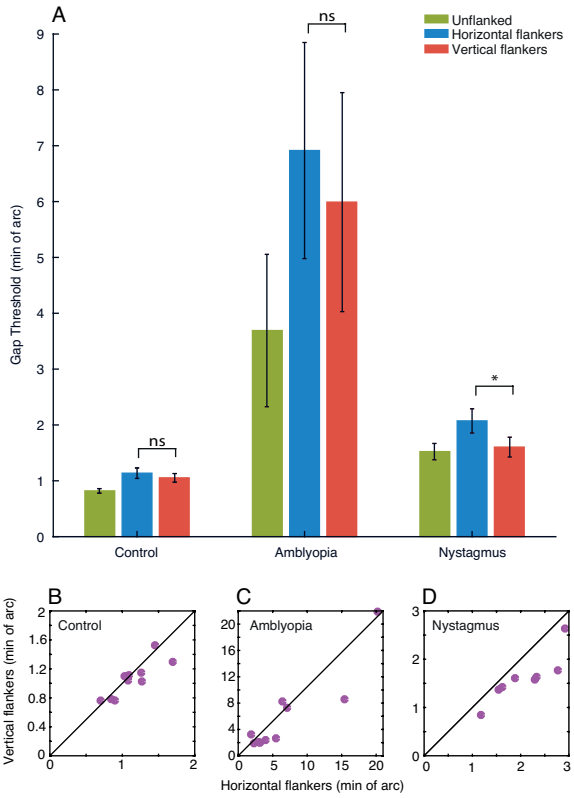

*Figure 3. A. Gap thresholds for all participant groups, plotted in minutes of arc on the y-axis. The blue bars plot thresholds for the unflanked condition, green bars the horizontal flanker condition and red bars the vertical flanker condition. Error bars represent the SEM, with *= significant and ns = not significant. B-D. Gap thresholds with horizontal flankers for each individual plotted on the x-axis, against gap thresholds with vertical flankers on the y-axis. The black line represents perfect correspondence between gap thresholds with horizontal and vertical flankers. Purple circles represent individual participants. Note the variation in X and Y scales.*

To investigate this, we prepared a priori comparisons to test between the image motion or sensory deficit hypothesis regarding nystagmic crowding. We undertook paired sample t-tests comparing horizontal and vertical flanker conditions for each group. As shown in Figure 3A, there is no clear difference between horizontal flanker and vertical flanker thresholds in the control group and indeed this difference was not significant, $t_{(9)}$=1.728, p=0.118. Although the amblyopic group show higher horizontal flanker thresholds compared to vertical flanker thresholds on average, this difference was not significant, $t_{(9)}$=1.128, p=0.288. In contrast, for the nystagmats there is a clear difference in performance, with the horizontal flankers producing higher thresholds than vertical flankers, which was found to be significant $t_{(7)}$=4.372, p=0.003.

To further explore these differences, Figure 3B-D plots the relationship between the horizontal flanker and vertical flanker conditions for each individual. In this plot the black line represents a direct correspondence between the horizontal and vertical flanker thresholds. If an individual had no difference between the two stimulus conditions then they would lie on this line. However, if an individual had a worse horizontal flanker threshold they would lie below the unity line, and vice versa. In the control group, all individuals were clustered around the unity line, with no consistent difference between the two crowding conditions – 5/10 observers demonstrated higher thresholds with horizontal flankers than with vertical. In the amblyopia group, 7/10 participants had worse thresholds in the horizontal flanker condition (below the line of unity) compared to the vertical flanker condition. In other words, although thresholds were worse on average with horizontal flankers than with vertical, this was not wholly consistent amongst the

amblyopic participants. For the nystagmus group, all participants consistently had worse thresholds with horizontal flankers than in the vertical flanker condition, with all data points lying below the line of unity. This bias towards higher thresholds in the horizontal flanker condition in the nystagmus individuals supports the findings in the paired sample t-test, both of which follow the prediction of image motion as the basis for nystagmic crowding. In other words, our findings reveal stronger crowding in the horizontal flanker condition than the vertical flanker condition in the nystagmus group, suggesting that nystagmic eye movements (which are predominantly horizontal in movement) could be the cause of elevations in horizontal crowding.

The role of image motion in crowding

The above results are consistent with eye movements being the cause for the elevated foveal crowding in nystagmus. To further consider this relationship, the role of eye movements on gap thresholds was investigated for each stimulus condition. From our hypothesis, the elevated thresholds in the horizontal flanker condition may occur through either image smear (where target and flankers' smear into each other as the stimuli move across the retina) or the shift of stimuli into peripheral vision (relocation of the stimuli into peripheral retina where crowding is known to occur).

We first sought to characterise the properties of these eye movements. On the horizontal plane, overall eye position variability across all trials was lowest in the control group (mean of the standard deviation across trials = 0.61°), which increased slightly for the amblyopes (1.03°). By contrast, the largest instability in horizontal eye position was seen in the nystagmus group (1.65°). On the vertical plane, eye position variability was low for all three groups. For controls (mean of the standard deviation across trials = 0.76°) and amblyopes (1.17°), these values were similar to those on the horizontal plane. For nystagmats the variability was higher than controls and amblyopes (1.34°), but lower than the horizontal variability in their eye movements. The average velocity of the eye across all trials was slowest in the control group (7.8°/sec), which increased in the amblyopic group (11.7°/sec), and further again in the nystagmus group (26.2°/sec).

If nystagmic crowding is due to the image motion caused by these eye movements, then properties like variability, velocity, and the duration of foveation should correlate with gap-size thresholds. In other words, with increases in eye position variability and eye speed we should see an increase in the size of gap thresholds. Figure 4A plots individual gap thresholds against the standard deviation of the horizontal position of the eye for each participant group. The correlation between gap thresholds and the standard deviation of the horizontal eye position was not significant in any testing condition in the control participant group (unflanked $r_{(9)}$=-0.052, p=0.888, horizontal flankers $r_{(9)}$=0.043, p=0.906, and vertical flankers $r_{(9)}$=0.155, p=0.668). This was the same in the amblyopic group (unflanked $r_{(9)}$=-0.143, p=0.694, horizontal flankers $r_{(9)}$=0.003, p=0.995 and vertical flankers $r_{(9)}$=0.095, p=0.794) as well as the nystagmus group (unflanked $r_{(7)}$=0.001, p=0.997, horizontal flankers $r_{(7)}$=0.186, p=0.659 and vertical flankers $r_{(7)}$=-0.185, p=0.661). Similarly, there was no significant correlation between horizontal eye velocity and thresholds (Figure 4B) in the control group (unflanked $r_{(9)}$=0.255, p=0.476, horizontal flankers $r_{(9)}$=0.171, p=0.638 and vertical flankers $r_{(9)}$=0.180, p=0.618). This was the same in the amblyopic group (unflanked $r_{(9)}$=-0.113,

p=0.758, horizontal flankers $r_{(9)}$=0.380, p=0.279 and vertical flankers $r_{(9)}$=0.014, p=0.970) as well as the nystagmus group (unflanked $r_{(7)}$=0.042, p=0.923, horizontal flankers $r_{(7)}$=0.182, p=0.666 and vertical flankers $r_{(7)}$=-0.146, p=0.731). Finally, there were no significant correlations with gap thresholds for either the variability in vertical eye position or velocity (data not shown). Altogether, there is no association between gap thresholds and either variability in eye position or velocity.

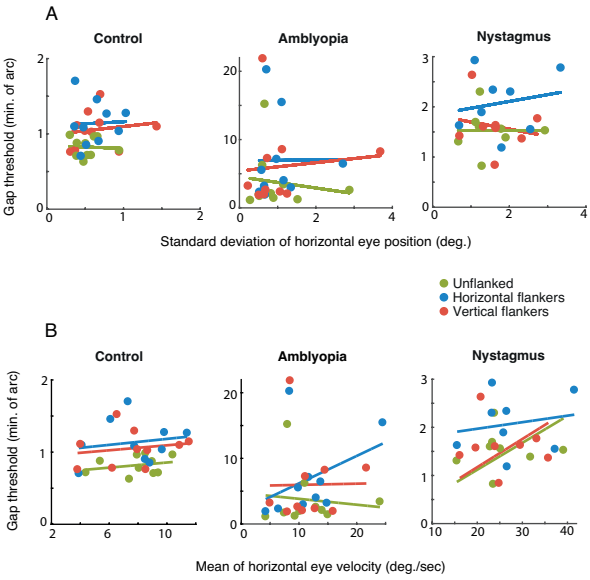

Figure 4. A. Gap thresholds plotted against the standard deviation of the horizontal eye position for each of the stimulus conditions and for each individual in the three participant groups (separate panels). B. Gap thresholds plotted against the mean of the eye velocity in the horizontal plane. Coloured circles separate the data into the three stimulus conditions (unflanked, horizontal and vertical flankers). Coloured lines represent the best fit linear function of the corresponding coloured data. Note the individual x and y axis scales for each participant group.

The role of foveation in crowding

Although eye position variability and velocity do not correlate with gap thresholds, these measures are somewhat crude estimates of the relationship between eye movements and the stimuli shown on screen. We next examined the effect of foveation duration in individual trials on performance. Foveation criteria were derived from the work of the Daroff-Dell'Osso lab (Dell'Osso & Jacobs, 2002), who observe that better measures of acuity are associated with a higher frequency and longer duration of foveation periods (Abadi & Worfolk, 1989; Cesarelli et al., 2000). As above, foveation is defined as a period where fixation is within a restricted spatial window around the target *and* where the velocity of the eye is lower than a cut-off value. To apply this to our data, we used parameters from the NAFX, where foveation was determined using eye positions within ±0.5-4° of the target and with a velocity below 4-10°/sec. We trialled different criteria within these ranges for position and velocity to define foveation and non-foveation periods, allowing us to establish the amount of time in each trial that met this range of foveation criteria. This allowed us to split trials into those with the longest foveation durations, termed 'best-foveation', and those with the shortest periods, termed 'worst-foveation', to determine whether an association can be found between foveation and gap thresholds.

To explore these criteria, Figure 5A shows the average amount of time within each trial classed as foveation within the different spatial windows, as defined by the parameters of the NAFX (i.e. between ±0.5-4°). Here, velocity was set at the lowest end of the NAFX criteria (4°/sec). Overall the control participants (red line) and amblyopes (green line) have comparable durations of time spent within the foveation window, both of which are longer in duration in comparison to the nystagmats (blue line), regardless of its size. Increasing the size of the spatial window gave a modest increase in foveation time, with all participant groups reaching a ceiling at a spatial window around 1.5-2°. Figure 5B shows the average duration of foveation

within the different velocity windows, once again determined by the NAFX (4-10°/sec), with the spatial window set at 2°. Again, the average duration of foveation is greatest for the controls and amblyopes, and considerably lower for the nystagmats. Increasing the window and allowing faster eye movements to be included increases the duration of foveation for all groups, though the nystagmats always show the least foveation. Although the precise amount of foveation varies depending on the parameters that are applied, nystagmats consistently show the least foveation in a given trial.

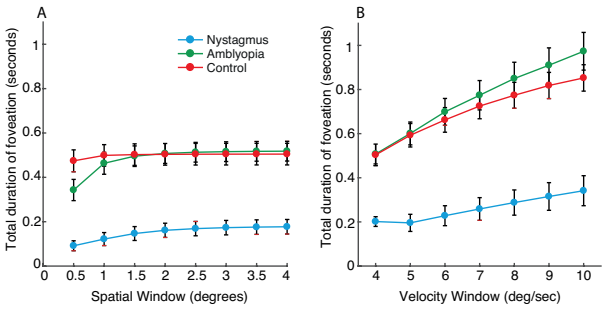

Figure 5. A. The average amount of time within each trial where the eye position falls within spatial windows of varying sizes around the target location (with a fixed velocity window), plotted separately for each of the participant groups. The X-axis shows the radius of the different spatial windows in 0.5° increments. The Y-axis is the total duration of time within the spatial window. B. The average duration of time spent within a range of foveation velocity windows (with a fixed spatial window). The X-axis shows the different velocity windows in 1°/sec increments, while the Y-axis shows the total duration of the trial within this window. Error bars represent the SEM.

We next divided these trials into best-foveation and worst-foveation categories, by first examining the distribution of foveation durations to find a combination of spatial and velocity windows that produced a normal distribution of durations across all trials, without any ceiling or floor effects. We found that parameters of ±2° for position and 8°/sec for velocity gave normal distributions for all nystagmus participants. We then applied these foveation criteria to data from all the nystagmic individuals to calculate the foveation duration within each trial. A median split was then applied to the data to identify trials with best-foveation and worst-foveation, resulting in 120 trials for each. The proportion of correct responses was then calculated for each gap size, separately for the best and worst foveation trials, and new psychometric functions were fit to calculate gap-size thresholds. If nystagmic crowding is caused by image motion, and in particular by foveation, we should find lower gap thresholds for all stimulus conditions (unflanked, horizontal and vertical flankers) and in particular a decrease in the difference between the horizontal flanker and vertical flanker stimulus conditions for best-foveation trials compared to the worst-foveation trials.

Figure 6 shows thresholds obtained from the best-foveation and worst-foveation trials for each stimulus condition in the nystagmus group. As in the main analysis, for each foveation condition, thresholds for the unflanked stimulus were lower than both horizontal and vertical flanker stimulus conditions, with an elevation of the horizontal flanker gap thresholds relative to the vertical flanker gap threshold. We compared our three stimulus conditions (unflanked, horizontal and vertical flankers) during trials with best-foveation and worst-foveation and undertook a 2x3 repeated measures ANOVA. The first factor was foveation and the second was stimulus condition. The ANOVA showed a significant main effect of stimulus condition $F_{(2,14)}= 14.329$, $p<0.001$, indicating that the stimulus condition being undertaken affected thresholds. The main effect for foveation was not significant, $F_{(1,7)}=0.343$, $p=0.58$, showing that thresholds were not affected by

whether the thresholds for nystagmus participants were derived from their trials with either best- or worst-foveation. The interaction between stimulus condition and foveation was not significant, $F_{(2,14)}=1.26$, $p=0.32$, again demonstrating that best-foveation or worst-foveation did not influence the pattern of thresholds between the stimulus conditions. The horizontal-elongation was present in both best- and worst-foveation conditions.

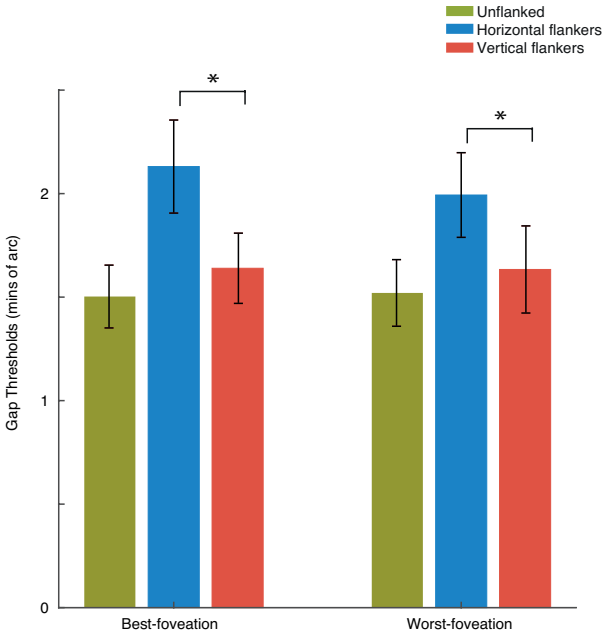

*Figure 6. Bar plot showing the average gap thresholds for the nystagmus participants split by best-foveation and worst-foveation trials. The data shows similar thresholds for within best-foveation and worst foveation for all stimulus conditions. A significant horizontal-elongation of crowding is seen in both best- and worst-foveation. Green bars represent the unflanked stimulus condition, blue bars the horizontal flanked condition and red bars the vertical flanked condition, *= significant and ns = not significant, error bars represent the SEM.*

Overall, our results have shown that thresholds for the unflanked and flanked conditions are elevated in nystagmus compared to typical adults, albeit to a lesser extent than the elevations seen with amblyopia. These deficits could be due to a long-term sensory change from poor visual input or due to the image motion induced by eye movements. Our findings of a significant difference between the gap thresholds measured in horizontal and vertical flanker conditions in the nystagmus group but not in the amblyopes and controls is consistent with the hypothesis that these deficits are caused by image motion through the momentary eye position changes. However, the lack of a correlation between gap-size thresholds and either the variability in eye position or eye velocity, as well as the lack of effect of foveation on thresholds, means that we cannot rule out a sensory deficit to nystagmic crowding. Although variations within the nystagmus group do not offer support for the image motion hypothesis, there are nonetheless large differences between the participant groups. It is possible that these large differences could cause the difference in crowding between the participant groups.

Experiment 2: Simulation of nystagmic crowding in typical vision

If nystagmic crowding is caused by image motion then the horizontal-elongation of crowding (where we find worse thresholds in the horizontal flanker condition compared to the vertical flanker condition) should be reproducible in typical adults when stimuli move on the screen in the same way as the eye movements of adults with nystagmus. In Experiment 2 we measured thresholds in the same stimulus conditions as above for adults with typical vision, either with stationary stimuli or with stimulus motion derived from the eye-movement recordings of the nystagmus group from Experiment 1. If image motion is the basis for nystagmic crowding then we should be able to see the same horizontal-elongation of crowding thresholds with this motion applied to the stimulus in

adults with typical vision. On the other hand, if nystagmic crowding is derived from a sensory deficit then the simple application of stimulus motion should fail to reproduce the observed elevations in thresholds and the horizontal-elongation of crowding.

Methods

Participants

Ten adults with typical vision (M_{age} = 31.4 years) were recruited, including one of the authors (JG). All participants wore full refractive correction if needed (M_{BCVA} = -0.10 logMAR) and were tested binocularly. No strabismus or nystagmus was present.

Stimuli and procedures

Participants underwent the same stimulus conditions as in Experiment 1 (unflanked, horizontal flankers and vertical flankers) with the same 4AFC Landolt-C orientation identification task. Presentation time for the stimulus was unlimited. Here, the 3 stimulus conditions were completed in 3 motion conditions. For the first 'no motion' condition, stimuli were static at the centre of the screen, as in Experiment 1. The latter two conditions had motion applied to the stimuli to simulate the pattern of nystagmus eye movements: in the motion-fixation condition the stimulus moved while participants fixated the centre of the screen, while for the motion-following condition participants were allowed to follow the stimulus as it moved. Pilot testing revealed the motion-fixation condition to be considerably more difficult than the motion-following condition; both were included here to allow measurement of performance at these different levels. Each block consisted of 60 trials and 5 practice trials as in Experiment 1, with each block repeated 3 times to give a total of 180 trials for each testing condition and motion condition. The same monitor, computer and EyeLink setup from Experiment 1 were used. In the no motion and motion-fixation conditions, fixation was monitored more closely, with a tolerable fixation zone of 1.5 degrees radius around the centre of the screen. If fixation deviated from the central fixation zone, the trial was cancelled and repeated at the end of the block. In the motion-following condition, trials were not cancelled when the eye diverged from this zone, though a given trial would not commence until fixation was within the central fixation zone in order to stop anticipation of the nystagmus waveform being presented.

Generation of the motion waveforms

In the two motion conditions, stimulus motion was derived from eye movements recorded from participants with nystagmus. These nystagmus waveforms were obtained from the 5-second central fixation recordings made during the 5-point calibration in Experiment 1. Because it has been shown that gaze position can alter the nystagmus waveform (Abadi & Whittle, 1991), the central fixation recordings (and not the eccentric locations) were used to reduce the possibility of altered nystagmus waveforms due to gaze position.

Sixty waveforms were selected after plotting all the waveforms and visually inspecting their quality, with a preference for recordings where the waveform was repeated regularly and without any loss of recording. Both horizontal and vertical elements of the waveforms were used. The initial 500ms of all trials were removed to counter any re-fixation movements to the central fixation position, leaving us with 4.5 second recordings. Waveforms were looped to provide a continuous movement, with an additional 500ms section added to the end that joined the end of the waveform to the beginning to allow a continuous loop. This was done by

linearly interpolating between the final eye position recording with the first recording. Creating a loop ensured continuous movement if the viewer took longer than 5 seconds to make their choice. An example recording is shown in Figure 7A. Because the original waveforms were recorded at 1000Hz, they were down-sampled to match the screen refresh rate of 60Hz, by sampling the recordings at every 17th interval (shown in Figure 7B). Once sampled in this way, the waveform was centred to pass through the central position of the screen by subtracting the mean position of the waveform. Centring the sampled waveform allowed us to ensure that the stimulus passed through the fovea at some point in the trial.

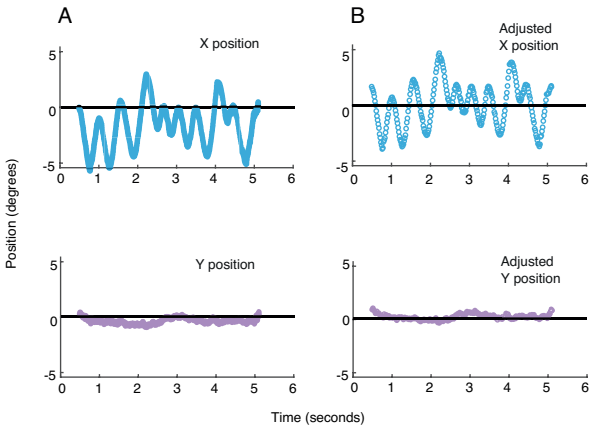

Figure 7. One example of a nystagmus waveform eye movement recording that was subsequently down-sampled and adjusted for the motion-fixation and motion-following conditions. (A) Top - original horizontal (X) position (blue circles) as a function of time, Bottom – original vertical (Y) position (lilac circles). (B) Top – X positions for the same waveform after it was down-sampled to every 17th position and centred (blue circles), Bottom – sampled and centred Y positions (lilac circles). Black line on each plot represents the centre of the screen.

Results

For each participant, stimulus condition (unflanked, horizontal flankers and vertical flankers) and motion condition (no-motion, motion-fixation and motion-following), three blocks of 60 trials were combined to give 180 trials per condition. Within each condition, the proportion of correct responses was determined for each stimulus size presented. Psychometric functions were fitted to the behavioural data for each stimulus condition and motion condition using a cumulative Gaussian function, as in Experiment 1, with thresholds again taken at 62.5% correct.

Figure 8A shows the average gap-size thresholds for all three stimulus conditions (unflanked, horizontal and vertical flankers) in each motion condition. In the no-motion condition, thresholds were low for the unflanked target (green bar) with slight elevations in thresholds with crowding when the horizontal and vertical flankers were introduced. This is similar to the threshold levels seen in Experiment 1 for the control group. In the motion-fixation condition, thresholds were elevated for all three stimulus conditions to a level that is greater than the thresholds found in Experiment 1 in the nystagmats, though lower than the amblyopes, with a particular elevation when flankers were present. In the motion-following condition (where the participant was allowed to follow the stimulus as it moved) we find again that thresholds were elevated relative to the no-motion condition, with further elevation in the flanked conditions. These elevations were of a lower magnitude than those of the motion-fixation condition and comparable to the level of performance seen for nystagmats in Experiment 1. Importantly, we see a similar horizontal-elongation of crowding thresholds for both motion-fixation and -following conditions, as for the nystagmats in Experiment 1.

A 3×3 repeated measures ANOVA was performed on thresholds with factors for stimulus condition and motion condition. We find a significant main

effect of stimulus condition $F_{(2,18)}$ = 44.334, p<0.001, a significant main effect of motion condition $F_{(2,18)}$ = 91.120, p<0.001 and a significant interaction between the stimulus and motion condition $F_{(4,36)}$ = 21.791, p<0.001. To determine the effect of motion on the horizontal-elongation of crowding we undertook paired samples t-tests between horizontal and vertical flanker conditions. We find no significant difference between the horizontal and vertical flanker conditions in the no-motion condition, $t_{(9)}$ = 0.203, p=0.844. The difference between crowding thresholds was however significant in the motion-fixation condition, with horizontally placed flankers producing more crowding than vertically placed flankers, $t_{(9)}$ = 3.177, p=0.011. However this was not significant in the motion-following condition $t_{(9)}$ = 1.596, p=0.145. This is seen in Figure 8B-D, where the black diagonal line represents the line of unity between thresholds with horizontal and vertical flankers. In the no motion condition all subjects cluster around the unity line showing no difference in crowding thresholds with either horizontal or vertical flankers. In contrast, for the motion-fixation and -following conditions we see a clear bias towards worse thresholds with horizontal flankers as all participants lie below the unity line.

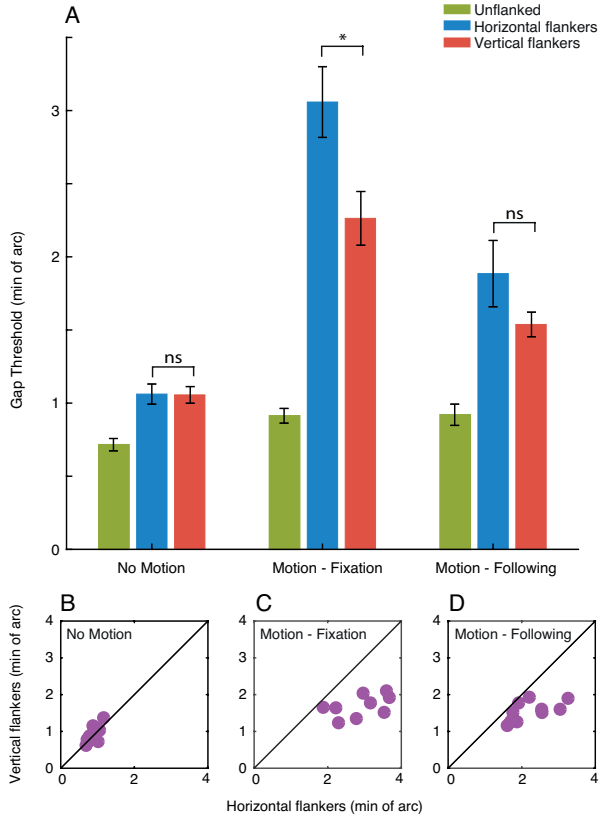

*Figure 8. A. Gap thresholds for Experiment 2, with all stimulus conditions (unflanked, horizontal and vertical flankers) tested in three motion conditions: no motion, motion-fixation and motion-following. The green bars represent the unflanked condition, blue bars represent horizontal flankers and the red bars represent vertical flankers along the x-axis. Gap thresholds are shown on the y-axis in minutes of arc. *= significant and ns = not significant, error bars represent the SEM. B-D. Horizontal flanker gap thresholds for each individual plotted on the x-axis against vertical flanker gap thresholds on the y-axis for the 3 motion conditions. The black line represents perfect correspondence between horizontal and vertical flanker thresholds. Purple circles represent individual participants, note the individual X and Y scales.*

Altogether, the introduction of nystagmic waveform motion to the stimulus does increase both unflanked and flanked thresholds with either horizontal or vertically placed flankers in adults with typical vision. We find larger elevations in crowding thresholds with horizontal flankers compared to vertically placed flankers when nystagmus motion is applied to the stimulus, similar to that found in the nystagmus group in Experiment 1. These findings of a horizontal-elongation of crowding support

our hypothesis that the image motion derived from eye movements could be the cause of nystagmic crowding. Interestingly however, the horizontal-elongation of crowding was only significant in the motion-fixation condition and not when participants were allowed to follow the stimulus with their eyes in the motion-following condition. The lack of significance in the latter might be due to individuals eye movements reducing the disruption caused by the image motion, or by reducing the shift of the stimulus into peripheral retina. In order to understand both this difference and the potential basis of nystagmic crowding, we next sought to associate properties of the image motion and associated eye movements (stimulus position, velocity, and periods of foveation) with the elevations in crowding thresholds.

Eye movement analysis

We first consider the broad properties of the eye movements made by participants in this experiment. Consistent with task requirements, the average variability of horizontal eye positions was greatest in the motion-following condition (0.12°±0.015°), where subjects followed the stimulus, compared to the no motion (0.08°±0.012°) and motion-fixation (0.09°±0.035°) conditions where fixation had to be maintained. Mean horizontal eye velocity was also greatest in the motion-following condition (7.69°/sec ±0.665°/sec) and lower in the no motion (6.30°/sec ±0.370°/sec) and motion-fixation (5.94°/sec ±0.710°/sec) conditions. Variability in vertical eye position was similar across the motion conditions: no motion (0.12°±0.009°), motion-fixation (0.11°±0.013°) and motion-following (0.14°±0.015°). Mean vertical eye velocity was lowest in the motion-fixation condition (6.63°/sec ±0.280°/sec), whereas the no motion and motion fixation condition were similar at 7.37°/sec ±0.412°/sec and 7.73°/sec ±0.421°/sec respectively. In other words, the motion-following condition generated a bias towards eye movements in the horizontal plane, which was not present in the motion-fixation and no motion conditions.

To fully account for the differences between these conditions, we also need to incorporate the stimulus motion into calculations. We first determined the absolute difference between the eye position relative to the stimulus throughout each trial. This was calculated by subtracting the stimulus position from the recorded eye position in both the horizontal and vertical plane. As expected, we find a low positional offset between the eye and stimulus in the horizontal plane for the no-motion condition (0.35°±0.020°), which increased once motion was applied (motion-fixation = 1.36°±0.005° and motion-following = 1.42°±0.014°). However, the similarity in positional offset for the latter two conditions does not account for the lower elevation in gap thresholds and the lack of horizontal-elongation of crowding found in the motion-following condition relative to motion fixation.

We next sought a more fine-grained analysis of the relationship between the stimulus and fixation using analyses of foveation duration, as in Experiment 1. In the course of these analyses, we noted a variability in the duration of trials across the three motion conditions. Average trial duration was longest in the motion-following condition (1.75±0.026secs), which decreased in the motion-fixation condition (1.37±0.007secs) and further again in the no-motion condition (1.05±0.011secs). The longer duration of trials in the motion-following condition could account for the observed improvements in both crowding tasks compared to the motion-

fixation group. However, it does not account for the lack of a significant horizontal-elongation in crowding.

In order to examine the duration of these trials where fixation fell within the foveation window, we again applied the spatial and velocity parameters from the NAFX to determine the foveation windows for position (±0.5-4°) and velocity (4-10°/sec). Figure 9A shows the average duration of foveation for a range of spatial windows from the NAFX, with the velocity parameter fixed at 4°/sec. As the spatial window widens from 0.5° to 4°, the duration of foveation increases in all three motion conditions. At the smallest spatial windows, foveation periods were longer in the no-motion condition compared to the two motion conditions. By increasing the spatial window of foveation, the motion conditions diverge, with motion-following having longer durations of foveation than motion-fixation. The longer periods of foveation for the motion-following condition with these intermediate spatial windows suggests that participants were indeed able to gain closer foveal proximity to the stimulus in periods of slower eye movements than in the motion-fixation condition where eye movements were not allowed. By shifting stimuli into the parafovea for longer durations, participants would gain a better judgement of the orientation of the Landolt-C, improving thresholds and reducing the horizontal-elongation of crowding relative to the motion-fixation condition. Importantly however, neither of the motion conditions allowed the degree of foveation present for the no-motion trial, particularly when foveation is defined using the narrowest spatial window. As in Experiment 1, we find little change in the average duration of foveation as velocity windows were widened (Figure 9B, where the spatial parameter was set at 2°).

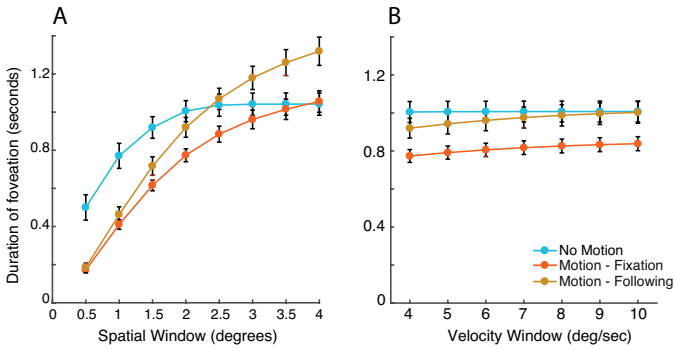

Figure 9. A. Average amount of foveation time across trials where the position of the eye falls within a spatial window around the target for each of the motion conditions (with a fixed velocity window). The X-axis show the different spatial windows in 0.5° increments. The Y-axis is the total duration of time within the spatial window. B. The average duration of time spent within the foveation velocity window (with a fixed spatial window). The X-axis show the different velocity windows in 1°/sec increments and the Y-axis is the total duration of the trial foveating. Error bars represent the SEM.

Overall, the results of Experiment 2 demonstrate that the application of nystagmus waveform motion to Landolt-C stimuli can produce a pattern of thresholds in adults with typical vision that is similar to that found in nystagmic crowding, both in terms of overall threshold elevation and the horizontal-elongation of crowding. This is likely due to a reduction in foveation duration, which would both cause both image smear and/or the relocation of the stimulus to more parafoveal locations.

Discussion

Our aim was to investigate the elevation in visual crowding associated with congenital idiopathic nystagmus, and whether it is the product of a long-term sensory deficit or due to the instantaneous image motion caused by the involuntary eye movements. In Experiment 1 we demonstrate foveal elevations in Landolt-C acuity and crowding for the nystagmus group

compared to typical adults, consistent with previous findings (Chung & Bedell, 1995; Pascal & Abadi, 1995). In the nystagmus group we further observe that thresholds were higher when flankers were positioned horizontally than vertically (horizontal-elongation of crowding), an effect that was absent for both typical adults and those with strabismic amblyopia. This suggests that the foveal crowding zone is elongated along the horizontal meridian in nystagmus, consistent with an origin in the image motion caused by the pattern of eye movements. In Experiment 2 we replicated these nystagmic crowding patterns, including the horizontal-elongation of crowding, in adults with typical vision using stimulus motion derived from the eye movements of participants with nystagmus. Thus, unlike the crowding effects that occur in typical and amblyopic vision, nystagmic crowding appears to be derived from image motion. We propose that the incessant eye movements of nystagmus cause either momentary image smear (which in turn could lead to either masking of the target by nearby flankers) or the relocation of the stimulus eccentrically into peripheral retina.

Our conclusion that nystagmic crowding results from the instantaneous eye motion is consistent with the results of Pascal and Abadi (1995), who found that crowding elevations were clearer in cases of idiopathic nystagmus than in those derived from albinism (despite the latter having higher mean elevations). They attributed the idiopathic crowding elevations to the shorter periods of foveation in the idiopaths, who tended towards jerk-type movements with large periods of retinal slip, compared to the albino group who had predominantly smooth pendular waveforms. In other words, the type of nystagmus waveform may be a determinant of nystagmic crowding. Accordingly, the idiopathic nystagmats tested here in Experiment 1 showed clear elevations in crowded thresholds, with a predominance of jerk-type nystagmus that gave only brief durations of foveation. The duration of foveation periods was also able to account for the different levels of crowding in typical adults with simulated nystagmus (Experiment 2) where reduced foveation durations were linked with increased elevations in crowding.

Prior examinations of the effect of image motion on visual acuity and crowding have met with mixed results. Falkenberg, Rubin, and Bex (2007) demonstrated that measures of acuity and crowding were unaffected by high levels of image instability, with random jitter used to mimic the fixation instability seen in patients with low vision. However, these levels of instability were lower than the variability in eye position seen in the nystagmats tested in the present study. Consistent with our findings, Chung and Bedell (1995) found elevations in crowding for control participants with simulated nystagmus, where repetitive jerk movements were applied to the stimulus. However, these elevations did not reach the same level as participants with nystagmus, with the greater degree of crowding in participants with nystagmus taken to reflect a long-term sensory deficit. In contrast, in Experiment 2 of the present study we replicated both the magnitude and pattern of nystagmic crowding (i.e. the horizontal-elongation of crowding) found in participants with nystagmus. It is possible that the type of motion applied to the stimuli could account for the difference between the studies. Chung and Bedell (1995) used idealised, repetitive waveforms that may have allowed participants to anticipate the stimulus movement, resulting in a

reduced elevation in crowding. Our use of directly measured nystagmus waveforms gave stimulus motion of greater variability that was clearly more disruptive to the task. This allowed us not only to replicate the magnitude of these elevations in typical adults, but also the horizontal-elongation of crowding, which follows the predominantly horizontal waveform of nystagmic eye movements.

The horizontal-elongation of crowding that we observe in nystagmus participants in Experiment 1 is consistent with anisotropies in the performance of those with nystagmus found in other tasks. Greater elevations in contrast detection and grating acuity have been found for vertical than horizontal gratings, in line with the disruptive effect of image smear along the axis of stimulus modulation (Abadi & King-Smith, 1979; Abadi & Sandikcioglu, 1975). Bisection acuity thresholds for participants with nystagmus have also been found to be worse for horizontal bisection acuity than vertical (Ukwade & Bedell, 2012), again consistent with image smear disrupting performance along the axis of stimulus modulation. Our observation of the horizontal-elongation of crowding with simulated nystagmus eye movements in typical vision is also consistent with previously simulated anisotropies. For instance, Ukwade and Bedell (2012) replicated their finding of an anisotropy for bisection acuity with repetitive simulated image motion. Our findings are perhaps also similar to the elongations in the spatial extent of crowding seen during smooth pursuit eye movements in those with typical vision (Harrison, Mattingley, & Remington, 2013). Interestingly, an anisotropy in horizontal vs. vertical crowding is also known to affect peripheral crowding, with greater disruption from horizontally placed flankers compared to vertically placed flankers in oblique locations of the visual field (Feng, Jiang et al. 2007). This anisotropy is not normally evident in foveal vision however, as we show in Experiment 1 and the no-motion condition of Experiment 2.

In the case of amblyopia, we also replicate the finding of Levi and Carney (2011) that there is no difference in the strength of crowding with horizontal or vertically placed flankers in the amblyopic fovea. This symmetry of elevated horizontal and vertical thresholds is consistent with these amblyopic deficits deriving from a sensory deficit, potentially related to findings of enlarged population receptive field sizes (Clavagnier et al., 2015). In the present study, the magnitude of the elevations in crowding in those with amblyopia was also substantially higher than those with either nystagmus or simulated nystagmus, again consistent with the presence of a sensory deficit for amblyopia but not for nystagmus.

We have argued that nystagmic crowding results from image motion. However, there are several aspects to image motion that may produce this deficit. One aspect of image motion produced by nystagmus that could give rise to crowding is the image smear caused by the eye movements. Eye movements could cause the target and flankers to smear into each other as the stimulus moves across the retina, hindering the ability to identify the orientation of the gap in the target Landolt C. Although this would produce crowding-like effects, the interference from the flankers in this case could be more closely linked with masking, the impairment of target discriminability by another spatially-overlapping pattern (Breitmeyer & Ganz, 1976; Campbell & Kulikowski, 1966). Crowding and masking show distinct properties – for instance,

the critical spacing for masking is proportional to the size of the target whereas crowding is size invariant (Pelli et al., 2004). Masking also impairs both detection and identification of the stimuli, whereas crowding impairs only identification (Pelli et al., 2004). Although crowding can be distinguished from masking in both peripheral vision (Levi et al., 2002b) and amblyopia (Levi et al., 2002c), the same may not be true for nystagmic crowding if image smear were the sole basis for these deficits.

An alternative explanation of the effect of image motion on nystagmic crowding is a change in stimulus location. Given that nystagmus eye movements are mainly horizontal (Abadi & Bjerre, 2002), their effect would be to shift the stimulus to more peripheral locations along the horizontal meridian where elevations in crowding are larger than the fovea (Bouma, 1970). The radial/tangential anisotropy of peripheral vision would also produce stronger crowding in the horizontal dimension for these locations (Toet & Levi, 1992). For our simulation of nystagmus in Experiment 2, thresholds were higher and more anisotropic in the motion-fixation condition compared to the motion-following and no-motion conditions. Our analysis of the average time spent foveating showed a reduction in foveation duration for the motion-fixation condition at intermediate spatial window sizes relative to both motion-following and the no-motion condition. In other words, better performance was obtained in conditions where participants could get closer to the stimulus for longer periods of time. This may also be true for the nystagmats in Experiment 1, who had lower foveation durations than those with typical vision. It is possible that those with nystagmus might base their judgements on the target stimulus when it is in peripheral vision, elevating crowding thresholds and giving rise to horizontal-elongation of crowding simply due to this peripheral location.

Conclusions

Overall our study has demonstrated elevated visual crowding in the fovea of participants with idiopathic nystagmus. These crowded elevations were higher with horizontal flankers than vertical flankers (horizontal-elongation of crowding), matching the horizontal bias of the nystagmus eye movements. Both these elevations in visual crowding and the horizontal-elongation of crowding were replicated in participants with typical vision when stimuli were moved to simulate the pattern of nystagmus. These results, and the dependence of thresholds on foveation duration, suggest that nystagmic crowding is driven by the eye movements relocating the stimulus into peripheral vision, where crowding is known to occur, rather than from a long-term sensory deficit. As a consequence, stabilisation of the eye movements in people with idiopathic nystagmus may provide a benefit to visual function by reducing these visual crowding effects.

Acknowledgments

The research was funded by Moorfields Eye Charity (GR000074) and the UK Medical Research Council (MR/K024817/1) and supported by the NIHR Biomedical Research Centre at Moorfields Eye Hospital NHS Foundation Trust. We thank Dr Alexandra Kalpadakis-Smith for her help with development of the experiment code.

Appendix

Appendix 1 – Clinical Characteristics for participants in Experiment 1.

	Age	RVA	LVA	BEO	Cover test	Eye Movements	Head posture	Stereopsis	Nystagmus type
	(years)	(logMAR)						(seconds of arc)	
Nystagmus	39	0.6	0.6	0.6	NAD	-	FTR	300	Jerk Right
	19	0.3	0.2	0.2	NAD	-	FTL	85	Pendular
	26	0.5	0.5	0.5	NAD	-	FTR HTL	300	Jerk Right
	34	-0.1	-0.1	-0.1	NAD	-	-	170	Jerk Left
	38	0.2	0.2	0.2	NAD	-	-	110	Jerk Right
	28	0.4	0.4	0.3	NAD	-	-	300	Pendular
	20	0.6	0.6	0.6	NAD	-	-	85	Jerk Left
	38	0	0	0	NAD	-	FTL	85	Jerk Right
Amblyopia	35	-0.2	0.3	-0.2	LCS	-	-	170	-
	49	0.1	0.8	0.1	LXT	-	-	-	-
	25	0.58	0	0	RCS	-	-	-	-
	43	0.2	-0.2	-0.2	RXT	-1 RLR	-	-	-
	34	0.3	-0.1	-0.2	RXT	-0.5 LMR	-	-	-
	36	-0.1	0.5	-0.1	LCS	-2 LMR	-	-	-
	25	0	0.8	0	LCS L/R	-1 Left Elevation	-	-	-
	36	0.3	-0.1	-0.1	RCS	-	-	-	-
	33	1	0	0	LCS	-1 BLR	-	-	-
	46	0	0.8	0	LXT	-	-	-	-
Control	36	0	0	0	NAD	-	-	55	-
	34	0	0	0	NAD	-	-	55	-
	28	0	0	0	NAD	-	-	55	-
	27	-0.1	-0.1	-0.1	NAD	-	-	85	-
	26	0	-0.1	-0.2	NAD	-	-	85	-
	39	-0.2	-0.2	-0.2	NAD	-	-	85	-
	21	-0.1	-0.1	-0.1	NAD	-	-	85	-
	41	0.1	0.1	0.1	NAD	-	-	85	-
	29	0	-0.1	-0.2	NAD	-	-	85	-
	40	-0.2	-0.2	-0.2	NAD	-	-	85	-

Table 1. Clinical characteristics of all participants. Key terms: RVA = right visual acuity, LVA = left visual acuity, BEO = both eyes open, NAD = no apparent deviation, L FA = left fully accommodative esotropia, LXT = left exotropia, RCS = right convergent squint, RXT = right exotropia, LCS = left convergent squint, RLR = right lateral rectus, LMR = left medial rectus, BLR = bilateral lateral rectus, FTR = face turn right, FTL = face turn left, HTL = head tilt left.

References

Abadi, R., & Bjerre, A. (2002). Motor and sensory characteristics of infantile nystagmus. *British Journal of Ophthalmology, 86*, 1152-1160.

Abadi, R., & King-Smith, P. (1979). Congenital nystagmus modifies orientational detection. *Vision Research, 19*(12), 1409-1411.

Abadi, R., & Sandikcioglu, M. (1975). Visual resolution in congenital pendular nystagmus. *American Journal of Optometry Physiological Optics, 52*(9), 573-581.

Abadi, R., & Whittle, J. (1991). The nature of head postures in congenital nystagmus. *Journal Archives of Ophthalmology, 109*(2), 216-220.

Abadi, R., & Worfolk, R. (1989). Retinal slip velocities in congenital nystagmus. *Vision Research, 29*(2), 195-205.

Barrett, B., Bradley, A., & McGraw, P. (2004). Understanding the neural basis of amblyopia. *Journal The Neuroscientist, 10*(2), 106-117.

Bedell, H. (2000). Perception of a clear and stable visual world with congenital nystagmus. *Optometry & Vision Science, 77*(11), 573-581.

Bouma, H. (1970). Interaction Effects in Parafoveal Letter Recognition. *Nature, 226*(5241), 177-178.

Brainard, D. (1997). The Psychophysics Toolbox. *Spatial Vision, 10*(4), 433-436.

Breitmeyer, B., & Ganz, L. (1976). Implications of sustained and transient channels for theories of visual pattern masking, saccadic suppression, and information processing. *Psychological review, 83*(1), 1.

Campbell, F., & Kulikowski, J. (1966). Orientational selectivity of the human visual system. *The Journal of Physiology, 187*(2), 437-445.

Cesarelli, M., Bifulco, P., Loffredo, L., & Bracale, M. (2000). Relationship between visual acuity and eye position variability during foveations in congenital nystagmus. *Documenta Ophthalmologica, 101*(1), 59-72.

Chung, S., & Bedell, H. (1995). Effect of Retinal Image Motion on Visual Acuity and Contour Interaction in Congenital Nystagmus. *Vision Research, 35*(21), 3071-3082.

Clavagnier, S., Dumoulin, S., & Hess, R. (2015). Is the cortical deficit in amblyopia due to reduced cortical magnification, loss of neural resolution, or neural disorganization? *Journal of Neuroscience, 35*(44), 14740-14755.

Coates, D., Levi, D., Touch, P., & Sabesan, R. (2018). Foveal crowding resolved. *Scientific Reports, 8*(1), 1-12.

Dell'Osso, L. (2002). Development of new treatments for congenital nystagmus. *Annals NY Academy Sciences, 956*, 361-379.

Dell'Osso, L., & Jacobs, J. (2002). An expanded nystagmus acuity function: intra- and intersubject prediction of best-corrected visual acuity. *Documenta Ophthalmologica, 104*(3), 249-276.

Dell'Osso, L., van der Steen, J., Steinman, R., & Collewijn, H. (1992). Foveation dynamics in congenital nystagmus. I: Fixation. *Documenta Ophthalmologica, 79*(1), 1-23.

Dickinson, C., & Abadi, R. (1985). The influence of nystagmoid oscillation on contrast sensitivity in normal observers. *Vision Research, 25*(8), 1089-1096.

Dunn, M., Harris, C., Ennis, F., Margrain, T., Woodhouse, M., McIlreavy, L., et al. (2019). An automated segmentation approach to calibrating infantile nystagmus waveforms. *Behavior research methods, 51*(5), 2074-2084.

Engbert, R., & Kliegl, R. (2003). Binocular coordination in microsaccades. In J. Hyona, R. Radach & H. Deubel (Eds.), *The Mind's Eyes: Cognitive and Applied Aspects of Eye Movements.* Oxford: Elsevier.

Falkenberg, H., Rubin, G., & Bex, P. (2007). Acuity, crowding, reading and fixation stability. *Vision Research, 47*(1), 126-135.

Feng, C., Jiang, Y., & He, S. (2007). Horizontal and vertical asymmetry in visual spatial crowding effects. *Journal of Vision, 7*(2), 13.11-10.

Flom, M., Heath, G., & Takahashi, E. (1963). Contour interaction and visual resolution: contralateral effects. *Science, 142*(3594), 979-980.

Greenwood, J., Bex, P., & Dakin, S. (2009). Positional averaging explains crowding with letter-like stimuli. *Proceedings of the National Academy of Sciences of the USA, 106*(31), 13130-13135.

Greenwood, J., Szinte, M., Sayim, B., & Cavanagh, P. (2017). Variations in crowding, saccadic precision, and spatial localization reveal the shared topology of spatial vision. *Proceedings of the National Academy of Sciences of the USA, 114*(17), E3573-E3582.

Greenwood, J., Tailor, V., Sloper, J., Simmers, A., Bex, P., & Dakin, S. (2012). Visual acuity, crowding, and stereo-vision are linked in children with and without amblyopia. *Investigative Ophthalmology & Vision Science, 53*(12), 7655-7665.

Guo, S., Reinecke, R., Fendick, M., & Calhoun, J. (1989). Visual pathway abnormalities in albinism and infantile nystagmus: VECPs and stereoacuity measurements. *Journal of pediatric ophthalmology & strabismus, 26*(2), 97-104.

Harrison, W., & Bex, P. (2015). A unifying model of orientation crowding in peripheral vision. *Current Biology, 25*(24), 3213-3219.

Harrison, W., Mattingley, J., & Remington, R. (2013). Eye movement targets are released from visual crowding. *Journal of Neuroscience, 33*(7), 2927-2933.

Kalpadakis-Smith, A., Tailor, V., Dahlmann-Noor, A., & Greenwood, J. (2017). The perceptual effects of visual crowding in amblyopic, developing, and peripheral vision. *Perception, 46*(10), 1228-1229.

Kalpadakis-Smith, A., Tailor, V., Dahlmann-Noor, A., Schwarzkopf, D., & Greenwood, J. (2018). The acuity and crowding deficits in strabismic amblyopia are stronger in the fovea than the visual periphery. *Investigative Ophthalmology & Visual Science, 59*(9), 5960-5960.

Kiorpes, L., & McKee, S. (1999). Neural mechanisms underlying amblyopia. *Current opinion in neurobiology, 9*(4), 480-486.

Levi, D. (2008). Crowding--an essential bottleneck for object recognition: a mini-review. *Vision Research, 48*(5), 635-654.

Levi, D., & Carney, T. (2011). The effect of flankers on three tasks in central, peripheral, and amblyopic vision. *Journal of Vision, 11*(1), 10-10.

Levi, D., Hariharan, S., & Klein, S. (2002b). Suppressive and facilitatory spatial interactions in peripheral vision: peripheral crowding is neither size invariant nor simple contrast masking. *Journal of Vision, 2*(2), 167-177.

Levi, D., Hariharan, S., & Klein, S. (2002c). Suppressive and facilitatory spatial interactions in amblyopic vision. *Vision Research, 42*(11), 1379-1394.

Levi, D., & Klein, S. (1985). Vernier acuity, crowding and amblyopia. *Vision Research, 25*(7), 979-991.

Liu, L., & Arditi, A. (2000). Apparent string shortening concomitant with letter crowding. *Vision Research, 40*(9), 1059-1067.

McKee, S., Levi, D., & Movshon, J. (2003). The pattern of visual deficits in amblyopia. *Journal of Vision, 3*(5), 380-405.

Papageorgiou, E., McLean, R., & Gottlob, I. (2014). Nystagmus in childhood. *Pediatric Neonatology, 55*(5), 341-351.

Parkes, L., Lund, J., Angelucci, A., Solomon, J., & Morgan, M. (2001). Compulsory averaging of crowded orientation signals in human vision. *Nature Neuroscience, 4*(7), 739.

Pascal, E., & Abadi, R. (1995). Contour interaction in the presence of congenital nystagmus. *Vision Research, 35*(12), 1785-1789.

Pelli, D. (1997). The VideoToolbox software for visual psychophysics: transforming numbers into movies. *Spatial Vision, 10*(4), 437-442.

Pelli, D., Palomares, M., & Majaj, N. (2004). Crowding is unlike ordinary masking: Distinguishing feature integration from detection. *Journal of Vision, 4*(12), 12-12.

Petrov, Y., & Meleshkevich, O. (2011). Asymmetries and idiosyncratic hot spots in crowding. *Vision research, 51*(10), 1117-1123.

Rosengren, W., Nyström, M., Hammar, B., & Stridh, M. (2020). A robust method for calibration of eye tracking data recorded during nystagmus. *Behavior Research Methods, 52*(1), 36-50.

Sarvananthan, N., Surendran, M., Roberts, E., Jain, S., Thomas, S., Shah, N., et al. (2009). The Prevalence of Nystagmus: The Leicestershire Nystagmus Survey. *Investigative Ophthalmology & Visual Science, 50*, 5201-5206.

Song, S., Levi, D., & Pelli, D. (2014). A double dissociation of the acuity and crowding limits to letter identification, and the promise of improved visual screening. *Journal of Vision, 14*(5), 3-3.

Theodorou, M. (2006). Predicting visual acuity in early onset nystagmus. *Seminars in Ophthalmology, 21*(2), 97-101.

Toet, A., & Levi, D. (1992). The two-dimensional shape of spatial interaction zones in the parafovea. *Vision Research, 32*(7), 1349-1357.

Ukwade, M., & Bedell, H. (1999). Stereothresholds in persons with congenital nystagmus and in normal observers during comparable retinal image motion. *Vision Research, 39*(17), 2963-2973.

Ukwade, M., & Bedell, H. (2012). Spatial-bisection acuity in infantile nystagmus. *Vision research, 64*, 1-6.

Watson, A., & Pelli, D. (1983). QUEST: A Bayesian adaptive psychometric method. *Perception & psychophysics, 33*(2), 113-120.